Aeroelastic Stability of the 747/Orbiter

J. Peter Reding* and Lars E. Ericsson†
Lockheed Missiles & Space Company, Inc., Sunnyvale, Calif.

A quasisteady analysis of the aeroelastic stability of the lateral (antisymmetric) modes of the 747/Orbiter vehicle demonstrates that the interference effect of the Orbiter wake on the 747 tail furnishes an aerodynamic undamping contribution to the low-frequency elastic modes. Likewise, the upstream influence of the 747 tail and aft fuselage on the Orbiter beavertail tail fairing also is undamping. Fortunately, these undamping effects cannot overpower the large damping contribution of the 747 tail, and the yaw modes are damped for the configurations analyzed.

Nomenclature

A = axial force; coefficient $C_A = A/\rho U^2 S/2$
B = $\rho U^2 S/2\,\bar{m}$
b = wingspan
c = reference length (mean aerodynamic chord)
D = damping derivative
$f(t)$ = buffeting force input
I = Orbiter inclination
K = spring constant
M = Mach number
$\bar{m}$ = generalized mass
n = yawing moment; coefficient $C_n = n/(\rho U^2 Sb/2)$
q = dynamic pressure
$q(t)$ = normalized coordinate
r = yaw rate
S = reference area
t = time
U = freestream velocity
$\bar{U}$ = convection velocity
x = axial coordinate
Y = yaw force; coefficient $C_Y = Y/(\rho U^2 S/2)$
z = lateral coordinate
α = angle of attack
β = sideslip angle
Δ = increment
δ = modal deflection
δr = rudder deflection
λ = wavelength
ξ = nondimensional axial coordinate, $\xi = x/c$
ζ = structural damping as a fraction of critical
ω = circular frequency
ϕ = modal deflection
ϕ' = mode slope

Subscripts

a = attached flow
O = Orbiter base
s = separated flow
T = 747 tail
u = upstream
w = wake
∞ = freestream
0 = $\beta = 0$

Superscripts

i = induced, e.g., $\Delta^i C_N$ = separation-induced normal force

Derivative symbols

ϕ' = $\partial\phi/\partial x$
$\dot{q}$ = $\partial q/\partial t$; $\ddot{q} = \partial^2 q/\partial t^2$
C_{n_δ} = $\partial C_n/\partial\delta$; $C_{Y_\beta} = \partial C_Y/\partial\beta$
$C_{n_{\dot\beta}}$ = $\partial C_n/\partial(b\dot\beta/2U)$; $C_{n_r} = \partial C_n/\partial\,(br/2U)$

Introduction

THE first of the shuttle configurations to fly will be the 747/Orbiter. The Orbiter is carried aloft atop a 747 airplane and launched for the initial approach and landing tests. Typical 747/Orbiter configurations are shown in Fig. 1. Early studies of the straight-wing, fully recoverable, shuttle booster indicated the possibility of aerodynamic undamping of the low-frequency yaw modes (Fig. 2).[1,2] The undamping was caused by the sidewash of the Orbiter wake on the carrier vehicle tail. This causes some concern for the aeroelastic stability of the 747/Orbiter. Lockheed Missiles & Space Company, Inc., was given the task of applying the same quasisteady techniques to the 747/Orbiter which were used so successfully in the aeroelastic analysis of the Apollo-Saturn.[3,4] The following summarizes the results of this analysis. It should be emphasized that this analysis is dependent upon static aerodynamic data as an input and, therefore, is deficient where experimental data are not available. References 5 and 6 are the sources of the aerodynamic data used.

Aerodynamic Interference Effects

The Orbiter effectively steers the flow forward of the 747 tail, as illustrated in Fig. 3. This steering induces a crossflow over the tail which is proportional to the Orbiter yaw angle β_0. Thus, the interference load is $\Delta^i C_{Y_{\beta w}}\beta_0$. Dynamically, the crossflow at the tail lags the Orbiter yaw attitude by an increment $\Delta\beta = \dot\beta\Delta t$, where $\Delta t = (x_T - x_O)/\bar{U}$. $\bar{U}$ is the convection speed in the Orbiter wake, and $(x_T - x_O)$ is the distance from the Orbiter base to the 747 tail. This wake-directing effect is directly analogous to the wake-directing effect of the Apollo escape rocket.[3,4]

In addition to the induced load on the 747 tail, there is the usual local attitude (β_T)-dependent load (Fig. 3). This load is simply $(C_{Y_{\beta s}}\beta_T)$, where

$$C_{Y_{\beta s}} = C_{Y_\beta}(q_w/q_\infty) \tag{1}$$

C_{Y_β} is the tail effectiveness in the freestream (Orbiter off), and q_w/q_∞ is the wake-to-freestream dynamic pressure ratio.

Presented as Paper 77-116 at the AIAA 15th Aerospace Sciences Meeting, Los Angeles, Calif., Jan. 24-26, 1977; submitted March 14, 1977; revision received June 21, 1977.
Index categories: Aeroelasticity and Hydroelasticity; Nonsteady Aerodynamics; Jets, Wakes, and Viscid-Inviscid Flow Interactions.
*Research Specialist. Member AIAA.
†Consulting Engineer. Associate Fellow AIAA.

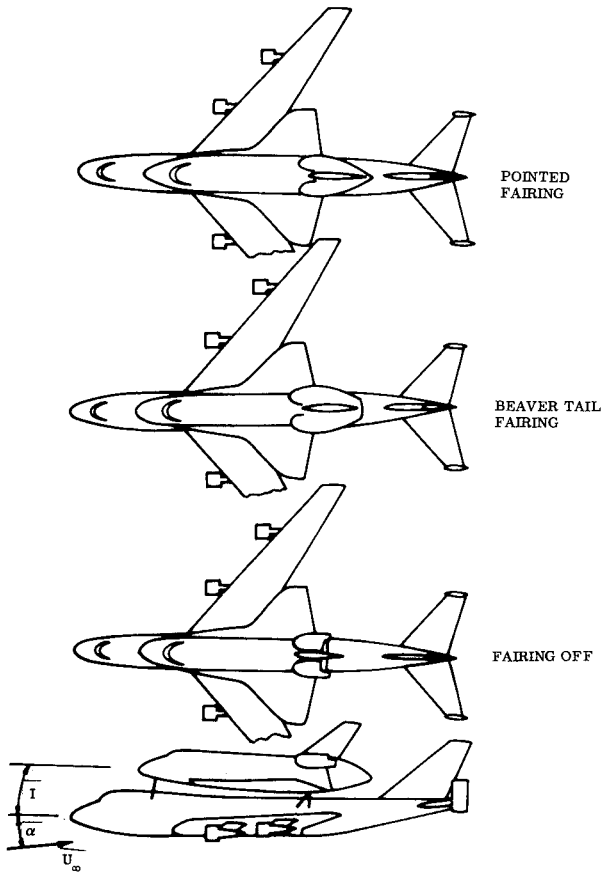

Fig. 1 747/Orbiter configurations.

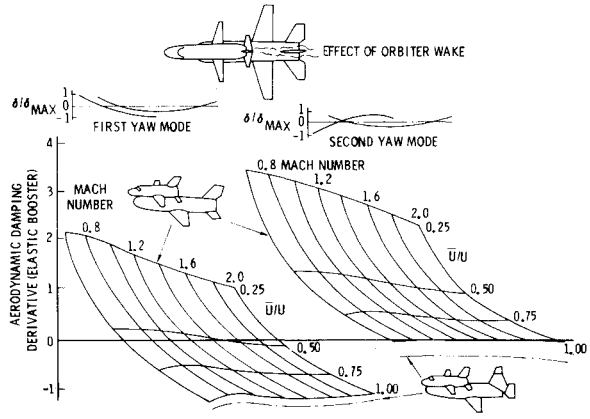

Fig. 2 Yaw damping of straight-wing booster.

The dynamic pressure ratio has been successfully related to the aerodynamic coefficient ratio. In the case of the Apollo-Saturn, the axial force ratio was found to be indicative of the dynamic pressure ratio, i.e., $q_w/q_\infty = C_{A0w}/C_{A0}$. However, this is not an effective indicator for the 747 tail, since differences in the tail increments between Orbiter-on and Orbiter-off approach the magnitude of the data accuracy. The rudder effectiveness was judged to be a better indicator of the dynamic pressure ratio; thus, $q_w/q_\infty = (C_{Y\delta r})_w/C_{Y\delta r}$. The total Orbiter sideforce derivative on the tail is the sum of induced and local derivatives:

$$C_{Y\beta} = C_{Y\beta s} + \Delta^i C_{Y\beta w} \tag{2}$$

The convection velocity ratio is simply

$$\bar{U}/U_\infty = (q_w/q_\infty)^{1/2} \tag{3}$$

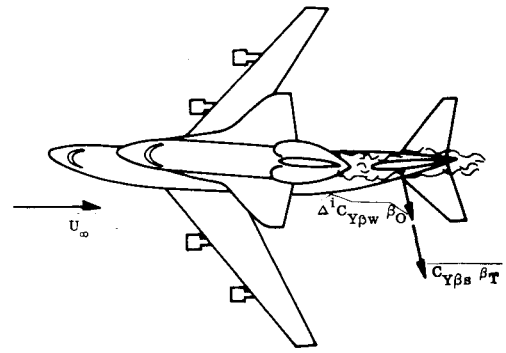

Fig. 3 747/Orbiter aerodynamic interference.

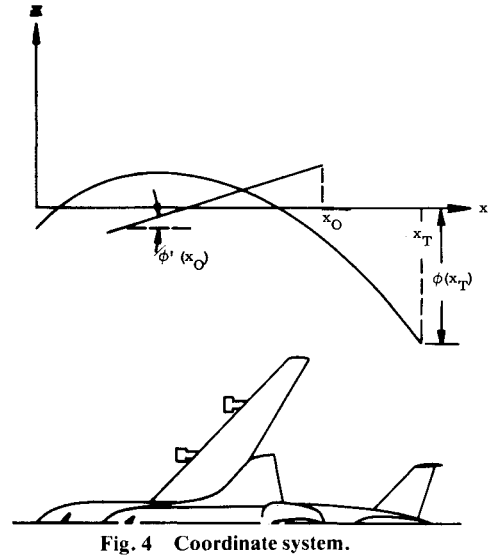

Fig. 4 Coordinate system.

Although this tacitly assumes incompressible flow, it was found to give a good approximation to the measured Apollo escape rocket wake convection speed.[7] This is probably because the bulk of the wake flow is of low speed and hence incompressible. This should be an even better estimate for the slender 747 tail, since it is buried almost completely in the low-velocity wake core.

Aerodynamic Damping

The equation of motion of an elastic vehicle describing single-degree-of-freedom bending oscillations can be written as follows[3,4]:

$$\ddot{q}(t) + 2\omega[\zeta - (B/2\omega U)(D_s + D_a)]\dot{q}(t)$$

$$+ \omega^2[1 - (B/\omega^2)(K_s + K_a)]q(t) = f(t) \tag{4}$$

where $B = \rho U^2 S/2\tilde{m}$, and $f(t)$ is the buffeting force input. D_s and D_a are the aerodynamic damping derivatives for separated and attached flows, respectively, where a negative value denotes damping. Multiplication by $-B/2\omega U = -\rho US/4\omega\tilde{m}$ puts the aerodynamic damping into the same form as the structural damping. The mode is stable if the $\dot{q}$ coefficient is positive, i.e.,

$$\zeta - (B/2\omega U)(D_s + D_a) \geq 0 \tag{5}$$

The separated flow damping derivative D_s for the 747/Orbiter is the sum of local and induced loads on the 747 tail and has been derived from Ref. 3 using the coordinate system of Fig. 4:

$$D_s = -C_{Y\beta s}[\phi(\xi_T)]^2$$

$$-\Delta^i C_{Y\beta w}\phi(\xi_T)\phi'(\xi_O)(U/\omega) \quad \sin(\omega\Delta t) \tag{6}$$

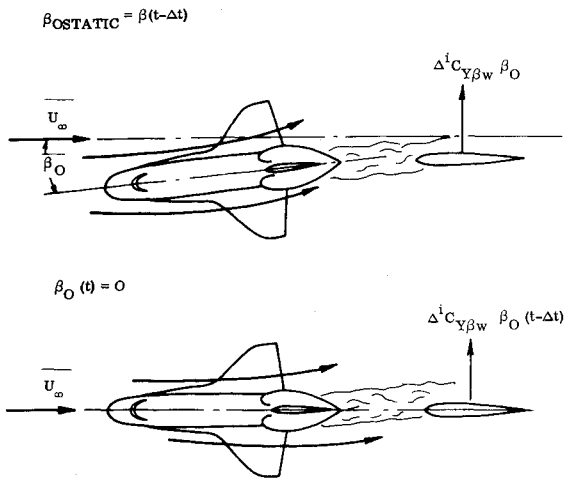

Fig. 5 Quasisteady loads on 747 tail.

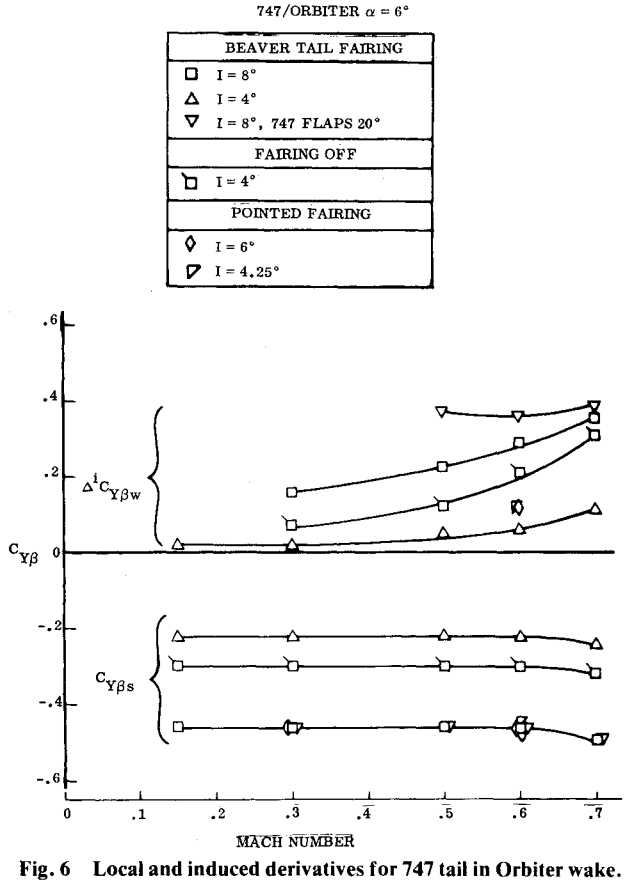

Fig. 6 Local and induced derivatives for 747 tail in Orbiter wake.

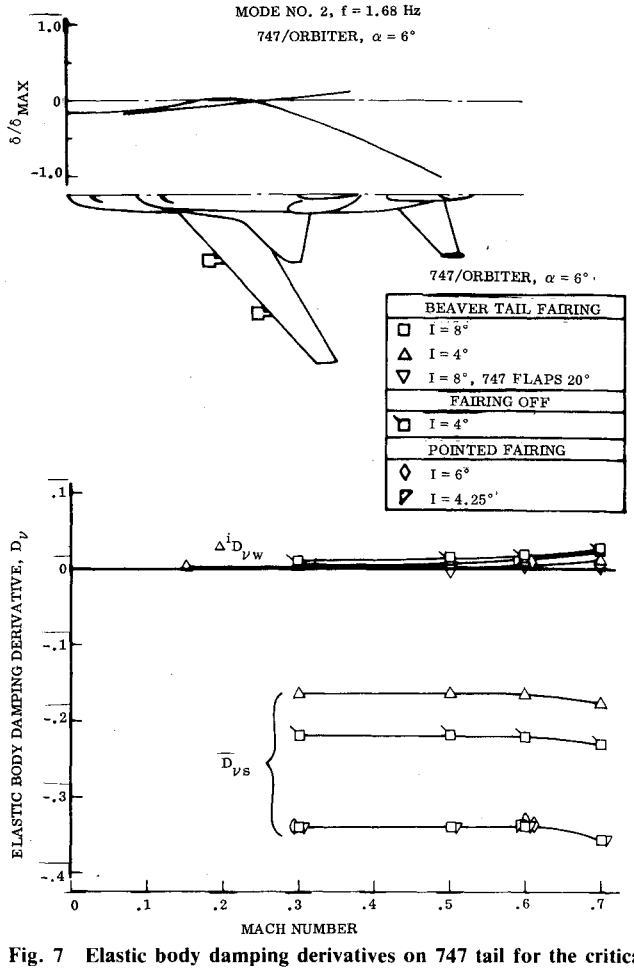

Fig. 7 Elastic body damping derivatives on 747 tail for the critical antisymmetric mode.

The attached flow damping derivative D_a is obtained from first-order momentum theory,[8] modified by use of the experimental values of $C_{Y\beta}$ for both Orbiter and 747.[3,4] From Eq. (6) and Fig. 4, one can see that the contribution of the induced derivative to D_s is undamping (positive) for the positive, statically stabilizing $\Delta^i C_{Y\beta w}$, since $\phi(\xi_T)$ and $\phi'(\xi_O)$ have opposite signs. This is illustrated in Fig. 5. Consider the Orbiter and 747 tail deflected in some mode as shown in the upper sketch. By virtue of its yaw angle β_O, the Orbiter induces a load on the 747 tail ($\Delta^i C_{Y\beta w}\beta_O$) which tends to return the tail to its null position. The interference effect is, therefore, statically stabilizing. As the Orbiter and tail pass through the null position during the modal oscillation (lower sketch), a residual load occurs on the tail, $\Delta^i C_{Y\beta w}\ \beta_O\ (t-\Delta t)$, which was generated at an earlier time $(t-\Delta t)$ when the Orbiter yaw angle was $\beta_O\ (t-\Delta t)$. This residual load is in the direction of motion, thus driving the oscillation; i.e., it is undamping.

Local and induced loads on the 747 tail have been extracted from wind-tunnel data for the 747/Orbiter.[5,6] Figure 6 shows that the load induced by the Orbiter wake ($\Delta^i C_{Y\beta w}$) is of the same order of magnitude as the load due to local crossflow ($C_{Y\beta s}$). However, the effect of the Orbiter wake on the modal damping is negligible relative to the local crossflow effect (Fig. 7). Why the Orbiter-induced effect is so overpowered by local crossflow for the 747/Orbiter, although it dominated the straight-wing shuttle booster, can be seen in Fig. 8. The damping effect of local crossflow is proportional to the square of the modal deflection at the tail. Since the relative deflection of the 747 tail is three times that of the straight-wing booster tail, the 747 tail is an order of magnitude more effective as a damper. In addition to this interference via downstream communication through the Orbiter wake to the 747 tail, there are upstream communication effects from the 747 tail to the Orbiter tail cone.

The 747 tail and aft fuselage have an interference effect on the Orbiter tail fairing through the wake recirculation region which is similar to dynamic sting interference.[9,10] There are two wake-induced loads on the tail fairing. The first effect, the free wake effect, occurs because, when the forebody generates lift, the wake immediately behind the body is inclined relative to the freestream (Fig. 9). Thus, a pressure gradient exists across the wake which eventually turns it parallel to the freestream. The pressure gradient produces higher windward side wake neck pressures that, when convected upstream through the wake recirculation region, cause a separation asymmetry. The result is a statically stabilizing tail load, which, of course, is undamping. Such undamping near-wake interference was observed in the yaw damping data

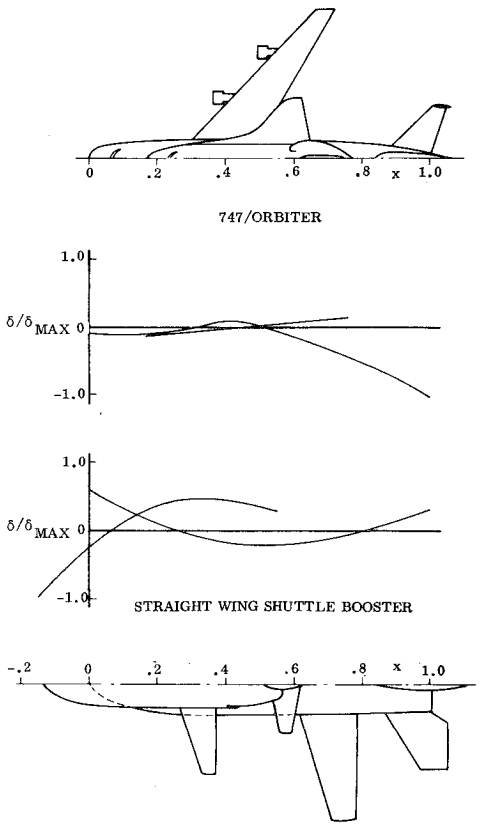

Fig. 8 Comparison of critical modes.

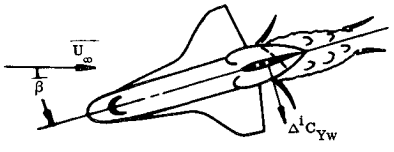

Fig. 9 Free near wake.

for the launch configuration with and without SRM's (Fig. 10).[11] An approximation to the yaw damping results was obtained[12] for the configuration with SRM's off simply by carpet-plotting the base increment from Ref. 13 to account for base radius and proximity to the sting flare and adding the increment to the first-order attached-flow damping estimate‡ (Fig. 10). The agreement with the experimental results is good when considering the possible effect of the Orbiter on the near-wake flow and the differences in sting configuration.§ The agreement for the configuration with SRM's on is not nearly as good, since the SRM's certainly alter the base flow.

The other induced load is analogous to the sting interference effect on a bulbous-based re-entry body (Fig. 11).[9,10] The sidewash of the Orbiter wake over the 747 tail results in unequal windward and leeward side wake neck pressures, which, when convected forward through the wake recirculation region, cause a separation asymmetry and an induced load on the tail fairing. The sense of this induced load depends upon the inclination of the tail relative to the Orbiter (β_T). These induced effects have a very long time lag, as they involve convection downstream from the Orbiter to the 747 tail and then upstream through the low-velocity recirculation region,[9,10] i.e.,

$$\Delta t_w = c(\xi_T - \xi_O)\,[\,(1/\bar{U}) + (1/\bar{U}_u)\,] \qquad (7)$$

‡The attached flow damping was estimated using first-order momentum theory[8] for a slender body. Static force measurements for the launch configuration were used to improve accuracy.

§The data of Ref. 11 were obtained using a symmetric flared sting of 13.14-deg total angle, whereas the data of Ref. 13 were obtained with a 12-deg asymmetric flared sting.

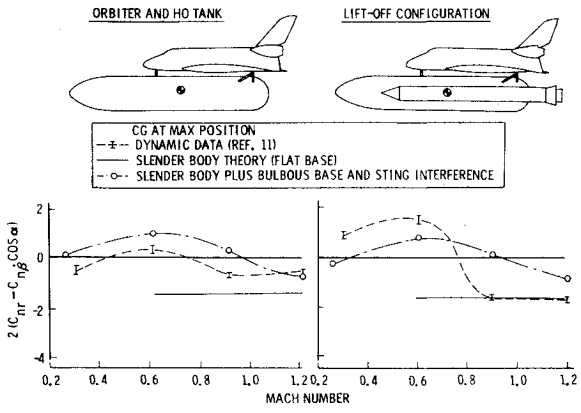

Fig. 10 Effect of HO tank bulbous base on launch configuration dynamic stability.

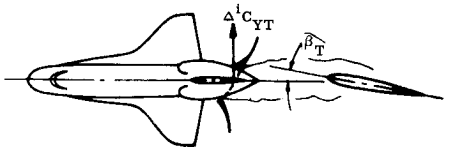

Fig. 11 Wake with submerged body.

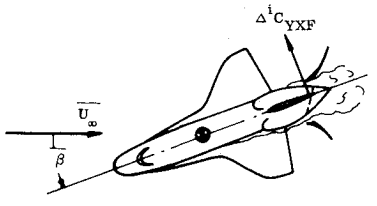

Fig. 12 Forebody crossflow effect on near wake.

where $\bar{U}$ and $\bar{U}_u$ are the downstream and upstream communication velocities, respectively.

Actually there is a third type of interference load occurring on the bulbous base (Fig. 9). The leeside boundary layer is weakened through forebody crossflow effects, allowing the separation to move upstream. The converse occurs on the windward side, resulting in a positive, statically destabilizing load (Fig. 12). Thus, the effect is to increase the Orbiter yaw damping.

Induced loads on the beavertail fairing have been extracted from the wind-tunnel data[5,6] as described in Ref. 14, with the time lag Δt_w taken from bulbous-based cone data.[9,10] Thus, a rough order-of-magnitude estimate of the 747 tail and aft fuselage interference on the modal damping was obtained. Figure 13 presents the damping components for mode 12, where the tail fairing loads are the most undamping. Although the effect of the 747 tail and aft fuselage produces an undamping effect on the beavertail fairing ($\Delta' D_{rTC}$), it is overpowered by the damping contributions of the Orbiter-less-tall-cone (principally the Orbiter tail), the 747 tail, and the 747 fuselage. There were only sufficient data on the beavertail tail fairing to allow an estimate of the tail fairing effects. Fortunately, this is the operational configuration. Thus, modal damping is assured for the critical mode 12.

The lumped-time-lag, quasisteady theory assumes that dynamically the instantaneous load distribution on a submerged body element is not substantially different from the static load distribution. It is not particularly significant how many cycles occur between the interference source and the submerged body unless other body elements are present which could alter the interference effect. This can be visualized from considering Fig. 14. The submerged 747 tail in Fig. 14a is well aft of the Orbiter and submerged in the Orbiter wake. The tail load can be expressed as a single lumped load, since the pertinent tail dimension c is small relative to the wavelength of

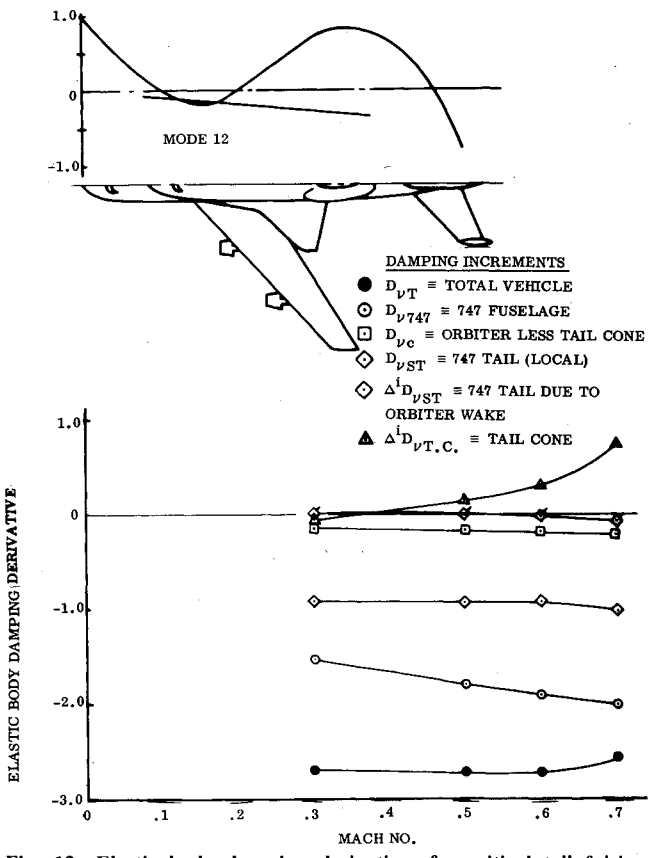

Fig. 13 Elastic body damping derivatives for critical tail fairing antisymmetric mode (No. 12, $f = 4.88$ Hz, beavertail fairing).

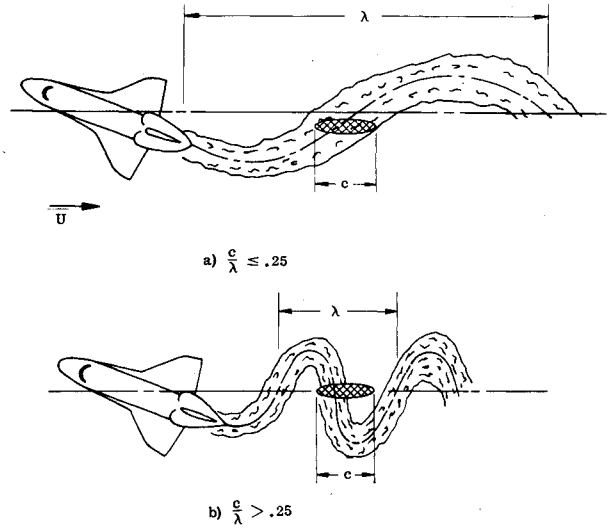

Fig. 14 Limit of quasisteady theory.

the oscillating wake, λ. However, when $\lambda \rightarrow c$ (Fig. 14b), one can see that the wake-induced crossflow at the rear of the tail will be altered by conditions at the leading edge, and the quasisteady technique breaks down. Thus, as long as $c/\lambda \leq 0.25$, the wave distortion will be minimal and the quasisteady theory is valid. Of course, this limit is not rigid, and the results will deteriorate gradually as one goes deeper into the questionable region, $c/\lambda > 0.25$. This limit of the quasisteady theory is indicated on Figs. 15 and 16, which present the modal damping results for the four critical antisymmetric modes. For modes 12 and 13, the quasisteady results begin to deteriorate at launch conditions (Fig. 16). However, at higher speeds ($M > 0.5$), where the induced loads are largest and, therefore, their undamping effects will be

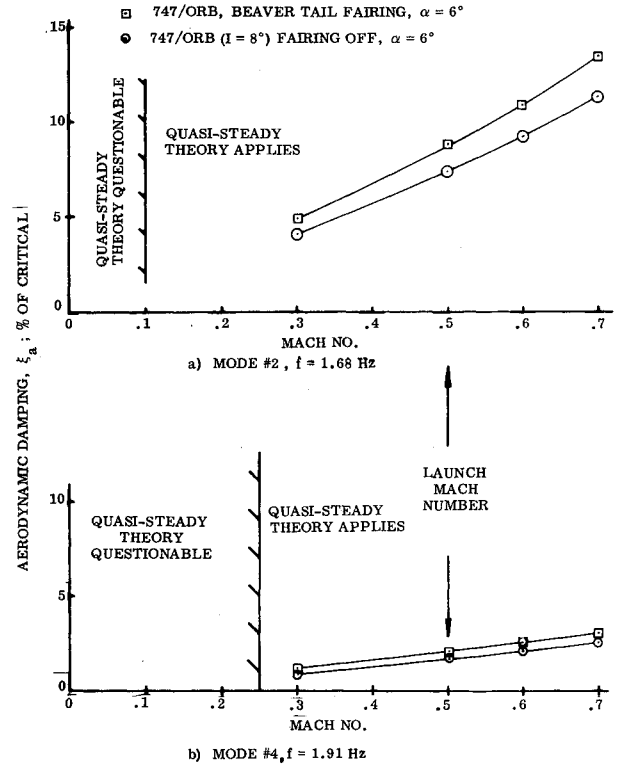

Fig. 15 Aerodynamic damping of launch modes 2 and 4.

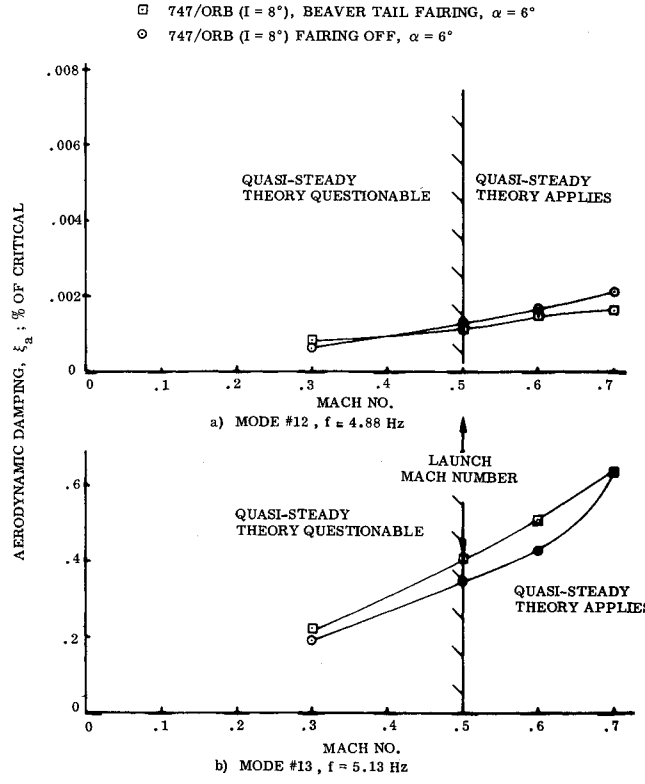

Fig. 16 Aerodynamic damping of launch modes 12 and 13.

largest, the quasisteady theory applies. Thus, it can be concluded that the yaw (antisymmetric) modes of the 747/Orbiter will be damped aerodynamically.

No estimate has been made yet of the damping of any of the symmetric or pitch plane modes. Comparison of 747 horizontal tail normal force increments indicates a significant downwash effect of the Orbiter on the horizontal tail (Fig. 17). The effect of Orbiter downwash is of the same order of

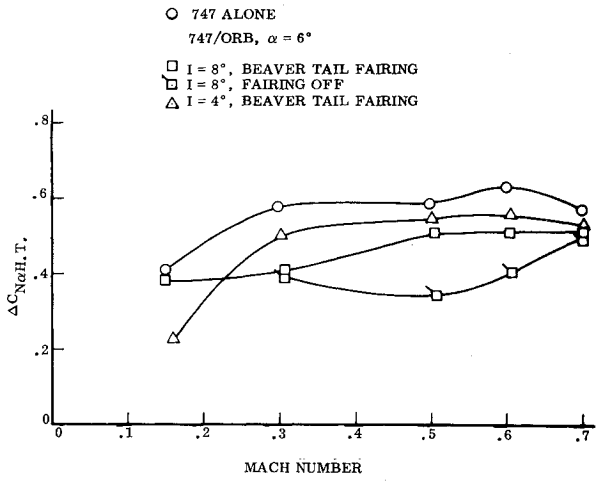

Fig. 17 Effect of Orbiter wake on 747 horizontal tail load.

magnitude as the sidewash effect considered previously. Furthermore, the interference effects on the tail fairing will be larger in the pitch plane than on the yaw plane for the flat beavertail configuration. It is, of course, still possible and even probable that the local crossflow effects at the tail will dominate the pitch modes as they did the yaw modes, and that the pitch modes, therefore, will be damped. Furthermore, the wake-induced damping derivatives are negligible at low speed, becoming significant only for $M > 0.3$. Thus, the problem can be resolved by increasing speed gradually during the flight-test program.

Modal response measurements were obtained on the first captive flights flown during the first quarter of 1977. Unfortunately, an assessment of the modal damping has not been accomplished as yet. However, no divergent or self-sustained oscillations were encountered in flight which qualitatively substantiates the conclusion of this analysis that the antisymmetric modes (and probably also the symmetric modes) are damped.

Conclusions

A quasisteady analysis of the aeroelastic stability of four critical antisymmetric modes of the 747/Orbiter has shown that the modes are damped aerodynamically for the following configurations: 1) 747/Orbiter without tail fairing, and 2) 747/Orbiter with beavertail fairing. The analysis indicates that the interference effect of the Orbiter on the 747 tail and the upstream effect of the 747 tail and aft fuselage on the Orbiter tail fairing have an aerodynamic undamping influence on certain critical modes. Fortunately, the large modal deflection of the 747 tail causes the damping effect of the 747 tail to overpower these undamping effects for the modes analyzed. Subsequent captive flight tests have encountered no self-sustained or divergent oscillations, qualitatively confirming the predicted aeroelastic stability.

Acknowledgments

The results presented here were obtained in a study for NASA, Contract NAS 8-30652, under the direction of W. W. Clever, NASA Marshall Space Flight Center, and J. C. Young, NASA Johnson Space Center.

References

[1] Reding, J. P. and Ericsson, L. E., "Review of Delta Wing Space Shuttle Vehicle Dynamics," Lockheed Missiles & Space Co., LMSC/D243938, Oct. 1971.

[2] Reding, J. P. and Ericsson, L. E., "Unsteady Aerodynamics Could Dominate the Space Shuttle Booster Aeroelastic Stability," AIAA Paper 74-362, Las Vegas, Nev., April 17-19, 1974.

[3] Ericsson, L. E. and Reding, J. P., "Analysis of Flow Separation Effects on the Dynamics of a Large Space Booster," *Journal of Spacecraft and Rockets*, Vol. 2, July-Aug. 1962, pp. 481-490.

[4] Ericsson, L. E. and Reding, J. P., "Report on Saturn I – Apollo Unsteady Aerodynamics," Lockheed Missiles & Space Co., LMSC/A650215, Feb. 1964.

[5] "Results of a 0.03 Scale Aerodynamics Investigation of a Boeing 747 Carrier (Model No. AX1319-I-1) Mated with a Space Shuttle Orbiter (Model 45-0) Conducted in the Boeing Transonic Wind Tunnel (CA5)," NASA CR-141, 800, Aug. 1975.

[6] "Wind Tunnel Data for a 747 Carrier/Orbiter Configuration" unpublished Boeing data, July 31, 1975.

[7] Reding, J. P., "Partial Simulation of Elastic-Body Dynamics for the Upper Stage Apollo-Saturn Launch Vehicle," Lockheed Missiles & Space Co., LMSC M-37-67-4, Dec. 1967.

[8] Bisplinghoff, R. L., Ashley, H., and Halfman, R. L., *Aeroelasticity*, Addison-Wesley, Cambridge, Mass., 1952, pp. 418-419.

[9] Ericsson, L. E. and Reding, J. P., "Aerodynamic Effects of Bulbous Bases," NASA CR-1339, Aug. 1969.

[10] Reding, J. P. and Ericsson, L. E., "Dynamic Support Interference," *Journal of Spacecraft and Rockets*, Vol. 9, July 1972, pp. 547-553.

[11] Freeman, D. C. Jr., Boyden, R. P., and Davenport, E. E., "Subsonic and Transonic Dynamic-Stability Characteristics of the Space Shuttle Launch Vehicle," NASA TMX-3336, March 1976.

[12] Reding, J. P. and Ericsson, L. E., "Unsteady Aerodynamic Flow Field Analysis of the Space Shuttle Configuration, Part II: Launch Vehicle Aeroelastic Stability," Lockheed Missiles & Space Co., LMSC-D057194, April 1976.

[13] Adcock, J. B., "Some Experimental Relations Between the Static and Dynamic Stability Characteristics of Sting-Mounted Cones with Bulbous Bases," *Transactions of the 3rd Technical Workshop on Dynamic Stability Problems*, Paper 5, Vol. II, NASA Ames Research Center, Moffett Field, Calif., Nov. 4-7, 1968.

[14] Reding, J. P. and Ericsson, L. E., "Unsteady Aerodynamic Flow Field Analysis of the Space Shuttle Configuration, Part IV, 747/Orbiter Aeroelastic Stability," Lockheed Missiles & Space Co., LMSC-D057194, Contract NAS 8-30652, March 1976.